IEEE Access
Multidisciplinary | Rapid Review | Open Access Journal

Received July 20, 2019, accepted August 9, 2019, date of publication August 21, 2019, date of current version September 6, 2019.

Digital Object Identifier 10.1109/ACCESS.2019.2936511

A Multi-Antenna Spectrum Sensing Scheme Based on Main Information Extraction and Genetic Algorithm Clustering

JIAWEI ZHUANG[1], YONGHUA WANG[1,2], SHUNCHAO ZHANG[1], PIN WAN[1,3], AND CHENHAO SUN[1]

[1]School of Automation, Guangdong University of Technology, Guangzhou 510006, China
[2]State Key Laboratory of Management and Control for Complex Systems, Institute of Automation, Chinese Academy of Sciences, Beijing 100190, China
[3]Hubei Key Laboratory of Intelligent Wireless Communications, South-Central University for Nationalities, Wuhan 430074, China

Corresponding author: Yonghua Wang (sjzwyh@163.com)

This work was supported in part by the special funds from the central finance to support the development of local universities under Grant 400170044 and Grant 400180004, in part by the project supported by the State Key Laboratory of Management and Control for Complex Systems, Institute of Automation, Chinese Academy of Sciences under Grant 20180106, in part by the National Natural Science Foundation of China under Grant 61971147, in part by the Foundation of Key Laboratory of Machine Intelligence and Advanced Computing of the Ministry of Education under Grant MSC-201706A, in part by the School-Enterprise Collaborative Education Project of Guangdong Province under Grant PROJ1007512221732966400, in part by the Foundation of National and Local Joint Engineering Research Center of Intelligent Manufacturing Cyber-Physical Systems and Guangdong Provincial Key Laboratory of Cyber-Physical Systems under Grant 008, and in part by the higher education quality projects of Guangdong Province and Guangdong University of Technology.

ABSTRACT Spectrum sensing is an indispensable technology for cognitive radio networks, which enables secondary users (SUs) to discover spectrum holes and to opportunistically use under-utilized channels without causing interference to primary users. Aim at improving the sensing performance, a multi-antenna spectrum sensing scheme based on main information extraction and genetic algorithm clustering (MIEGAC) is proposed in this paper. Specifically, in order to reduce the amount of signal that is transferred to the fusion center, an information pre-processing scheme based on principal component analysis (PCA) is presented. Main information from the sensing signal is extracted via PCA, which reduces the cost of the reporting channel and the impact of interfering information on detection result. Furthermore, an information fusion method is described in this paper, which takes the place of complicated matrix decomposition algorithms. Moreover, inspired by machine learning, a clustering scheme based on genetic algorithm is introduced to classify signal features, which implements the spectrum sensing decision and avoids calculating the decision threshold. Simulation results illustrate that the MIEGAC can considerably improve the sensing performance for spectrum sensing. Significantly, this paper provides a novel approach for the design of centralized spectrum sensing algorithms in cognitive radio technologies.

INDEX TERMS Spectrum sensing, principal component analysis, information fusion, genetic algorithm clustering.

I. INTRODUCTION

As the rapid development of wireless communication technologies, it is key that spectrum resources are efficiently and reasonably utilized, particularly in the fifth generation (5G) communication networks [1]–[3]. In cognitive radio networks (CRN), spectrum sensing (SS) is a critical technology to effectively improve this problem that is insufficient utilization for spectrum resources [4]–[6]. However, conventional SS methods and technologies have some disadvantages. For instance, energy detection [7] has a poor sensing performance under uncertain noise. Moreover, matched filter detection [8] requires the prior information of primary users (PUs) and noise power. Furthermore, single antenna technologies have terrible quality of service and poor transmission rate [9]. Recently, with the advancement of SS technologies, multi-antenna SS technologies are proposed, which improve the capacity of wireless communication systems

The associate editor coordinating the review of this manuscript and approving it for publication was Mahdi Zareei.

and the detection performance [10], [11]. It is well known that cooperative sensing technologies that multiple secondary users (SUs) simultaneously detect the state of PUs are more reliable than single-node SS schemes [12]. Motivated by the above discussions, multi-antenna cooperative spectrum sensing (MCSS) is considered in this article.

A. PREVIOUS WORK

The previous couple of years has witnessed the prevalence of SS algorithms based on random matrix theory. These algorithms has solved some disadvantages of conventional SS schemes, which extract the eigenvalues via the sampling covariance matrix and used the distribution of the eigenvalues to calculate the decision threshold [13]. Moreover, these algorithms not only don't require the prior information of PUs and noise power, but also have good sensing performance under uncertain noise. Unfortunately, these algorithms based on random matrix theory tend to ignore other elements of the sampling covariance matrix when these eigenvalues of that matrix are obtained. It is worth noting that information geometry is a theory that studies statistical issues through modern differential geometry. And information geometry theory turns statistical issues into geometric issues, which intuitively analyzes statistical issues [14]. Thus, information geometry theory provides a novel idea for studying spectrum sensing methods. Specifically, in [15], the sampling covariance matrix was mapped onto the statistical manifold via information geometry tool; and then, the decision threshold was derived by the distance feature between the points on the manifold. However, the above schemes need to calculate the decision threshold as traditional sensing schemes do. And it is well known that a inaccurate decision threshold directly affects the sensing performance.

Surprisingly, some novel SS schemes based on machine learning algorithms can avoid calculating the decision threshold, since some complex issues and calculations may be solved well by machine learning [16], [17]. Usually, clustering algorithms are used in SS schemes, since clustering algorithms have excellent performance to analyze data and divide the received signal into different classes by the similarity of that signal [18]. For example, a sensing method that signal energy features were classified by K-means clustering algorithm was proposed in [19], which worked better than traditional energy detection. Moreover, two-dimensional signal feature vectors were constructed by IQ decomposition (IQ) or decomposition and reorganization (DAR), and these feature vectors were classified by K-means [20], [21]. Furthermore, three-dimensional signal feature vector was obtained by IQ and DAR, which was classified by K-means [22]. Obviously, these mentioned algorithms have better sensing performance than conventional SS schemes based on random matrix theory. On the other hand, some SS algorithms based on information geometry theory were proposed, such as [23] and [24]. In [23], a scheme based on information geometry and DAR was proposed, which used Fuzzy-c-means clustering algorithm to classify signal feature. In [24], a method based on information geometry and K-medoids clustering algorithm was proposed, which used empirical modal decomposition algorithm to denoise the sensing signal. Undoubtedly, all of the above SS schemes based on machine learning improve the sensing performance.

B. CONTRIBUTION

Given what has been discussed above, a multi-antenna spectrum sensing scheme based on main information extraction and genetic algorithm clustering (MIEGAC) is proposed in this paper. It is noted that SS schemes based on different clustering algorithms have different sensing performance [20]. Genetic algorithm (GA) is an optimized search algorithm that simulates natural evolution. And genetic algorithm clustering (GAC) works better than many non-GA-based clustering algorithms, such as K-means, K-medoids, Fuzzy-c-means, etc [25]. Therefore, choosing a suitable clustering algorithm may improve the sensing performance. Different from these algorithms based on literature [20] and [23], the MIEGAC uses GAC algorithm to classify signal features. Moreover, inspired by literature [26], an information fusion method is proposed to construct signal feature vector, which is different from these methods based on different matrix decomposition algorithms, such as IQ and DAR. Furthermore, many existing SS algorithms directly send the observed signal or the denoising signal to the fusion center (FC) [23], [24], which undoubtedly increase the cost of the reporting channel. And other schemes use hard fusion algorithm, which require SU to have complicated signal processing capability [27]. However, a pre-processing scheme based on principal component analysis (PCA) is proposed in the article, which decreases the cost of the reporting channel and only requires SUs to have simply processing capability. Different from the algorithm based on dimensionality reduction in the density space [28], this pre-processing scheme directly reduces the dimension of the sensing data. And the impact of PCA on spectrum sensing is discussed in the simulation section. Given what has been introduced above, the main contributions of this paper are summarized as follows:

1) A pre-processing scheme based on PCA is proposed in this paper. This scheme not only reduces the cost of reporting channel, but also doesn't require SUs to have complicated processing capabilities. Moreover, a lot of interfering signal is filtered after PCA.
2) An information fusion method is introduced to construct signal feature vectors, which can avoid complicated matrix decomposition, such as IQ and DAR.
3) A new decision algorithm based on GAC algorithm is proposed, which can avoid calculating the decision threshold. This algorithm makes the detection more accurate.
4) There are two conditions that are considered in experiments. One is that SU collects the sensing signal with the same SNR. Another condition is that SU gains the observed signal with a different SNR, owing to every SU has a different location.

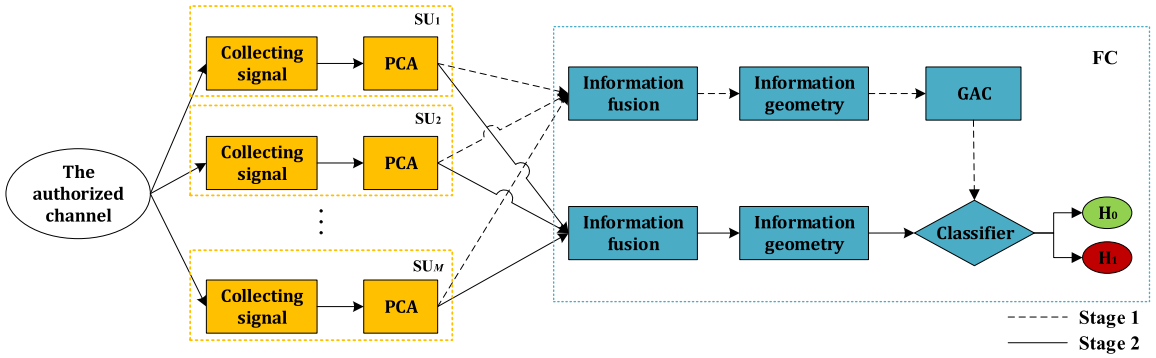

FIGURE 1. These basic processes of the MIEGAC.

These basic steps of the MIEGAC are drawn in Fig. 1. All SUs observe the authorized channel and collect the sensing signal. Then, SU extracts main information from the sensing signal and sends main information to the FC. In the FC, the stage 1 means the training processes. The GAC model is trained in advance and a classifier is obtained after training is completed. Particularly, this model does not train again. Furthermore, the stage 2 represents the actual sensing processes, including signal feature is obtained by information geometry and this classifier is used to classify signal feature.

The rest of this article is listed as follows. Section II introduces the MCSS scenario and signal model; and Section III describes the pre-processing algorithm based on PCA. In Section IV, an information fusion method and feature extraction method are presented. The GAC algorithm is described in Section V. Section VI shows simulation results and analysis; and conclusions are drawn in Section VII.

Conveniently, the symbols and meanings used in this article are explained in Table 1.

TABLE 1. Symbols and meanings.

Symbol	Meaning
H_0, H_1	PU signal is absent and present
α	Number of antennas
j	Number of SUs
$x^\alpha(t), x_j^\alpha(t)$	The observed signal at time t
$w^\alpha(t), w_j^\alpha(t)$	Gaussian white noise
$h^\alpha(t)$	Information gain
$s^\alpha(t), s(t)$	PU signal
A_{ab}	Correlation between the ath antenna and the bth antenna
d_{ab}	Distance between the ath antenna and the bth antenna
λ	Wavelength
θ	Propagation direction of antenna
$\mathbf{X}_j(t), \overline{\mathbf{X}}_j(t)$	The signal matrix
$\mathbf{R}$	Covariance matrix or a point on the manifold
$\mathbf{I}$	Unit matrix
μ_α, v_α	Eigenvalue and eigenvector
$p(g, \delta)$	Probability density function
g	Sample of random variables
$\mathbb{R}^n$	European space
Θ	The open set on the European space
$\overline{\mathbf{R}}$	Riemann mean
$\widehat{T}, \widetilde{T}$	Signal feature set
P_m	Probability of missed detection
P_f	Probability of false alarm
P_d	Probability of detection
ϑ	A parameter controls P_m and P_f

II. THE MCSS SYSTEM MODEL

A. THE MCSS SCENARIO

The MCSS scenario is shown in Fig. 2. This paper considers a simple cognitive radio network that consists of single PU and M SUs as well as a FC. Assume that both PU and the FC have one antenna, respectively; and SU has l antennas. All SUs are around the PU. Usually, SU observes the authorized channel and collects enough signal. And then, main information from the sensing signal is extracted through PCA and send to the FC. Finally, the FC detects whether the authorized channel is available.

B. SIGNAL MODEL

The SS problem can be abstracted as a binary hypothesis: the PU signal is present (H_1) or absent (H_0) [20], [21]. For a SU, based on the above assumptions, the corresponding mathematical model is given as

$$x^\alpha(t) = \begin{cases} w^\alpha(t), & H_0 \\ h^\alpha(t)s^\alpha(t) + w^\alpha(t), & H_1 \end{cases} \quad (1)$$

where $\alpha(\alpha = 1, 2, \ldots, l)$ indicates the αth antenna; $x^\alpha(t)$ represents the sensing signal observed by the αth antenna at time $t(t = 1, 2, .., N)$; $w^\alpha(t)$ denotes Gaussian white noise that obeys $\mathcal{N}(0, \sigma^2)$; $s^\alpha(t)$ represents the PU signal and is independent of the noise signal $w^\alpha(t)$; and $h^\alpha(t)$ indicates the information gain of the αth antenna [29]. In addition, the channel fading is not considered in the simulations, where $h^\alpha(t) = 1$.

In the MCSS scenario, the sampling signal between different antennas has a certain correlation. The correlation between the $a(a \in \alpha)$th antenna and the $b(b \in \alpha)$th antenna

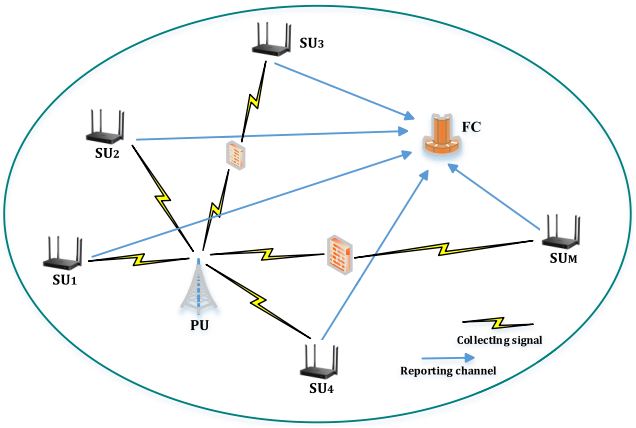

FIGURE 2. The MCSS scenario.

can be given by

$$A_{ab} = e^{-23\Omega^2(\frac{d_{ab}}{\lambda})}, \tag{2}$$

where $\Omega = \frac{\sqrt{\theta^2+2\cos\theta-2}}{2\theta}$; d_{ab} indicates the distance between the ath antenna and the bth antenna; λ represents the wavelength and θ denotes the propagation direction of antenna. The correlation is the greatest (i.e., A_{ab} is largest) when $\lambda = 2d_{ab}$ and $\theta \to 0$ *rad*; and it can be considered as an ideal condition that $s^a(t) = s^b(t) = s(t)$ [30]. Thus, under the ideal condition, the MCSS signal model based on (1) can be defined as

$$x_j^{\alpha}(t) = \begin{cases} w_j^{\alpha}(t), & H_0 \\ s(t) + w_j^{\alpha}(t), & H_1 \end{cases} \tag{3}$$

where $j(j = 1, 2, ..., M)$ means the jth SU; $x_j^{\alpha}(t)$ represents the sensing signal observed by the αth antenna of the jth SU; and $s(t)$ indicates the PU signal. Therefore, a $l \times N$ matrix that obtained by the jth SU can be expressed as

$$\mathbf{X}_j(t) = \begin{bmatrix} x_j^1(1) & x_j^1(2) & \cdots & x_j^1(N) \\ x_j^2(1) & x_j^2(2) & \cdots & x_j^2(N) \\ \vdots & \vdots & \ddots & \vdots \\ x_j^l(1) & x_j^l(2) & \cdots & x_j^l(N) \end{bmatrix}. \tag{4}$$

III. PRE-PROCESSING SCHEME BASED ON PCA

PCA is an important technique to process data. Its purpose is that removes redundancy via reducing dimensions of data and extracts important information of data [31]. Motivated by PCA, this paper proposes a new scheme that main information of the sensing signal is extracted after SU collects signal. Notably, this scheme can control the amount of main information through the parameter β. Thus, choosing a suitable parameter β is one of critical steps for the MIEGAC. Next, the following will introduce how PCA works.

Based on (4), a covariance matrix from the jth SU is given as follow:

$$\mathbf{R}_j = E[\mathbf{X}_j(\mathbf{X}_j)^H], \tag{5}$$

where $E[\cdot]$ represents mathematical expectation and $(\cdot)^H$ indicates complex conjugate transpose. Based on the assumption that the PU signal and the noise signal are independent of each other, (5) can be written as

$$\mathbf{R}_j = \mathbf{R}_s + \mathbf{R}_w. \tag{6}$$

In (6), $\mathbf{R}_s$ represents the PU signal covariance matrix; $\mathbf{R}_w$ indicates the noise signal covariance matrix. And $\mathbf{R}_w = \sigma_w^2\mathbf{I}$, where $\mathbf{I}$ denotes a unit matrix. Furthermore, (3) now becomes

$$\mathbf{R}_j = \begin{cases} \sigma_w^2\mathbf{I}, & H_0 \\ \sum_{\alpha=1}^{l}(\mu_\alpha - \sigma_w^2)v_\alpha v_\alpha^{\mathrm{T}} + \sigma_w^2\mathbf{I}, & H_1 \end{cases} \tag{7}$$

where μ_α means the αth eigenvalue of matrix $\mathbf{R}_j$ and v_α represents the αth eigenvector corresponding to the αth eigenvalue. Arranging these eigenvalues from large to small, we can obtain

$$\mu_1 \geq \mu_2 \geq \cdots \geq \mu_\beta \geq \mu_{\beta+1} = \cdots = \sigma_w^2. \tag{8}$$

Thus, we also obtain

$$\begin{cases} H_0 : \mu_1 = \mu_2 = \cdots = \mu_\beta = \mu_{\beta+1} = \cdots = \sigma_w^2, \\ H_1 : \mu_1 \geq \mu_2 \geq \cdots \geq \mu_\beta \geq \mu_{\beta+1} = \cdots = \sigma_w^2. \end{cases} \tag{9}$$

The larger eigenvalue is, the more obvious the signal feature will be [30]. Therefore, select β the largest eigenvalues and the rest are set to zero. For the jth SU, $\mathbf{X}_j$ is reconstructed into a $\beta \times N$ matrix $\overline{\mathbf{X}}_j$. $\overline{\mathbf{X}}_j$ is expressed as

$$\overline{\mathbf{X}}_j(t) = \begin{bmatrix} x_j^1(1) & x_j^1(2) & \cdots & x_j^1(N) \\ x_j^2(1) & x_j^2(2) & \cdots & x_j^2(N) \\ \vdots & \vdots & \ddots & \vdots \\ x_j^\beta(1) & x_j^\beta(2) & \cdots & x_j^\beta(N) \end{bmatrix}, \tag{10}$$

where $\beta \in [1, l]$. Consequently, important information is extracted by these above steps after the jth SU obtains the observed signal.

It is no difficult job for us to find that the parameter β can determine the size of matrix $\overline{\mathbf{X}}_j(t)$. And the size of matrix $\overline{\mathbf{X}}_j(t)$ indicates the amount of main information that is transmitted to the FC. Accordingly, a suitable parameter β can save the cost of the reported channel. For instance, SU sends the main signal collected by an antenna to the FC when $\beta = 1$. Moreover, SU sends all the sensing signal collected by all antennas to the FC when $\beta = l$. Furthermore, SU sends the main signal collected by β antennas to the FC when $\beta \in [1, l]$. Briefly, these basic processes of PCA algorithm are given in *Algorithm 1*.

Algorithm 1: PCA algorithm for the MIEGAC

Step 1. The signal matrix $\mathbf{X}_j$ from jth SU is constituted a covariance matrix $\mathbf{R}_j$ by (5).

Step 2. Calculate $\mathbf{R}_j$ to obtain the eigenvalues μ_α and the eigenvectors v_α.

Step 3. The eigenvalues μ_α are listed from large to small; select β the largest eigenvalues and the rest are set to zero.

Step 4. Reconstruct $\mathbf{X}_j$ into a new matrix $\overline{\mathbf{X}}_j$.

IV. SIGNAL FEATURES EXTRACTION

A. AN INFORMATION FUSION METHOD

There are some algorithms that use DAR or IQ to construct a two-dimensional signal feature vector [20], [23]. However, to avoid the complicated matrix decomposition algorithms, an information fusion method is used to obtain a two-dimensional feature vector. Specifically, the received signal is divided into two groups $\mathbb{Y}_1$ and $\mathbb{Y}_2$ according to the information fusion method. And the following will introduce the information fusion method.

Suppose that there are $M(M \geq 2)$ SUs. The received signal is given by

$$\mathbb{Y} = [\overline{\mathbf{X}}_1(t), \overline{\mathbf{X}}_2(t), \ldots, \overline{\mathbf{X}}_M(t)]^{\mathsf{T}}. \tag{11}$$

And $\mathbb{Y}$ is divided into $\mathbb{Y}_1$ and $\mathbb{Y}_2$ when M is even, where $\mathbb{Y}_1 = [\overline{\mathbf{X}}_1, \overline{\mathbf{X}}_3, \ldots, \overline{\mathbf{X}}_{M-1}]^{\mathsf{T}}$ and $\mathbb{Y}_2 = [\overline{\mathbf{X}}_2, \overline{\mathbf{X}}_4, \ldots, \overline{\mathbf{X}}_M]^{\mathsf{T}}$, respectively. Similarly, when M is odd and β is even, $\mathbb{Y}_1$ and $\mathbb{Y}_1$ can be expressed as

$$\mathbb{Y}_1 = [\overline{\mathbf{X}}_1, \overline{\mathbf{X}}_3, \ldots, \overline{\mathbf{X}}_{M-2}, \overline{\mathbf{X}}_M^{\frac{\beta}{2}}]^{\mathsf{T}} \tag{12}$$

and

$$\mathbb{Y}_2 = [\overline{\mathbf{X}}_2, \overline{\mathbf{X}}_4, \ldots, \overline{\mathbf{X}}_{M-1}, \overline{\mathbf{X}}_M^{\beta-\frac{\beta}{2}}]^{\mathsf{T}}, \tag{13}$$

respectively. Moreover, when both M and β are odd, $\mathbb{Y}_1$ and $\mathbb{Y}_2$ can be written as

$$\mathbb{Y}_1 = \begin{bmatrix} x_1^1(1) & x_1^1(2) & \cdots & x_1^1(N) \\ \vdots & \vdots & \vdots & \vdots \\ x_1^\beta(1) & x_1^\beta(2) & \cdots & x_1^\beta(N) \\ \vdots & \vdots & \vdots & \vdots \\ x_{M-2}^1(1) & x_{M-2}^1(2) & \cdots & x_{M-2}^1(N) \\ \vdots & \vdots & \vdots & \vdots \\ x_{M-2}^\beta(1) & x_{M-2}^\beta(2) & \cdots & x_{M-2}^\beta(N) \\ x_M^1(1) & x_M^1(2) & \cdots & x_M^1(N) \\ \vdots & \vdots & \vdots & \vdots \\ x_M^{\frac{\beta-1}{2}}(1) & x_M^{\frac{\beta-1}{2}}(2) & \cdots & x_M^{\frac{\beta-1}{2}}(N) \end{bmatrix} \tag{14}$$

and

$$\mathbb{Y}_2 = \begin{bmatrix} x_2^1(1) & x_2^1(2) & \cdots & x_2^1(N) \\ \vdots & \vdots & \vdots & \vdots \\ x_2^\beta(1) & x_2^\beta(2) & \cdots & x_2^\beta(N) \\ \vdots & \vdots & \vdots & \vdots \\ x_{M-1}^1(1) & x_{M-1}^1(2) & \cdots & x_{M-1}^1(N) \\ \vdots & \vdots & \vdots & \vdots \\ x_{M-1}^\beta(1) & x_{M-1}^\beta(2) & \cdots & x_{M-1}^\beta(N) \\ x_M^{\beta-\frac{\beta-1}{2}}(1) & x_M^{\beta-\frac{\beta-1}{2}}(2) & \cdots & x_M^{\beta-\frac{\beta-1}{2}}(N) \\ \vdots & \vdots & \vdots & \vdots \\ x_M^\beta(1) & x_M^\beta(2) & \cdots & x_M^\beta(N) \end{bmatrix}, \tag{15}$$

respectively.

After the received signal is divided into two groups, the covariance matrix $\mathbf{R}_1$ and $\mathbf{R}_2$ from $\mathbb{Y}_1$ and $\mathbb{Y}_2$ can be obtained, which are expressed as

$$\mathbf{R}_1 = E[\mathbb{Y}_1 \mathbb{Y}_1^H] \tag{16}$$

and

$$\mathbf{R}_2 = E[\mathbb{Y}_2 \mathbb{Y}_2^H], \tag{17}$$

respectively.

B. INFORMATION GEOMETRY THEORY

Definition 1: Define a set

$$\mathcal{M} = \{p(g, \delta) | \delta \in \Theta \in \mathbb{R}^n\}, \tag{18}$$

where $p(g, \delta)$ represents probability density function; g is a sample of random variables; Θ indicates the open set on the European space $\mathbb{R}^n$; the $\mathcal{M}$ denotes a statistical manifold when a differential structure is created in set $\mathcal{M}$; and δ means the coordinate on the statistical manifold [23]. On the $\mathcal{M}$, the probability distributions, $\mathcal{W}(n, \mathcal{L}_1)$ and $\mathcal{W}(n, \mathcal{L}_2)$, can be determined by $\mathcal{L}_1$ and $\mathcal{L}_2$, respectively, where $\mathcal{L}_1$ and $\mathcal{L}_2$ are positive definite matrices. According to information geometry theory, $PD(n, \mathbb{R})$ represents a positive definite matrix manifold, which is a manifold composed of all $n \times n$ positive definite symmetric matrices; and $SPD(n, \mathbb{R})$ is the tangent space of the manifold $PD(n, \mathbb{R})$ [32]. The statistical manifold can be described as $SPD(n, \mathbb{R})$, because the parameter space Θ of the zero-mean multivariate Gaussian distribution is isomorphic to $SPD(n, \mathbb{R})$.

Assume that there are two points, δ_c and δ_d, on the manifold, and there are multiple curves connecting these points. The geodesic means the shortest curve among these curves. And the Riemann distance is the length of the geodesic, which can be used to analyze the similarity between distributions. Thus, in the $SPD(n, \mathbb{R})$, the Riemann distance between two points can be defined as

$$\begin{aligned} \mathcal{D}^2(\mathbf{R}_c, \mathbf{R}_d) &= \| \log^2(\mathbf{R}_c^{-\frac{1}{2}} \mathbf{R}_d \mathbf{R}_c^{-\frac{1}{2}}) \| \\ &= \| \log(\mathbf{R}_c^{-1} \mathbf{R}_d) \|^2 \\ &= Tr[\log^2(\mathbf{R}_c^{-1} \mathbf{R}_d)] \\ &= \sum_{u=1}^{n} \log^2(\eta_u), \end{aligned} \tag{19}$$

where $\| \cdot \|$ means the Frobenius norm; $\mathbf{R}_c$ and $\mathbf{R}_d$ denote the coordinates of points on the manifold, respectively; $Tr[\cdot]$ represents the trace of matrix; and η_u indicates the uth eigenvalue of the matrix $\mathbf{R}_c^{-\frac{1}{2}} \mathbf{R}_d \mathbf{R}_c^{-\frac{1}{2}}$.

Suppose that there are multiple points on the manifold, in order to analyze the similarity between these points, we tend to use a reference point to calculate the Riemann distance. In addition, the Riemann mean is used to obtain the reference point. Assume that there are Q points, $\mathbf{R}_q (q = 1, 2, \ldots, Q)$, on the manifold, and the objective function of

the Riemann mean can be given by

$$\Phi(\mathbf{R}_q) = \frac{1}{Q}\sum_{q=1}^{Q}\mathcal{D}^2(\mathbf{R}_q, \overline{\mathbf{R}}), \tag{20}$$

where $\overline{\mathbf{R}}$ is a point on the manifold when $\Phi(\cdot)$ takes the smallest value. And $\overline{\mathbf{R}}$ can be expressed as

$$\overline{\mathbf{R}} = \arg\min \Phi(\overline{\mathbf{R}}). \tag{21}$$

There are two points, $\mathbf{R}_1$ and $\mathbf{R}_2$, on the manifold when $Q = 2$, and (21) can be written as

$$\overline{\mathbf{R}} = \mathbf{R}_1^{\frac{1}{2}}(\mathbf{R}_1^{-\frac{1}{2}}\mathbf{R}_2^{\frac{1}{2}}\mathbf{R}_1^{-\frac{1}{2}})^{\frac{1}{2}}\mathbf{R}_1^{\frac{1}{2}}. \tag{22}$$

It is noted that (22) is no longer applicable when $Q > 2$. Furthermore, the gradient descent algorithm is used to calculate $\overline{\mathbf{R}}$, which is given by

$$\overline{\mathbf{R}}_{h+1} = \overline{\mathbf{R}}_h^{\frac{1}{2}} e^{-\tau\sum_{q=1}^{Q}\log(\overline{\mathbf{R}}_h^{-\frac{1}{2}}\mathbf{R}_q^{\frac{1}{2}}\overline{\mathbf{R}}_h^{-\frac{1}{2}})}\overline{\mathbf{R}}_h^{\frac{1}{2}}, \tag{23}$$

where $\tau(\tau > 0)$ indicates the speed of iteration; and h represents the numbers of iteration. The Riemann mean $\overline{\mathbf{R}} = \overline{\mathbf{R}}_{h+1}$ when the gradient descent algorithm is successful. The gradient descent method is given in *Algorithm 2*.

Algorithm 2: The gradient descent algorithm is used to calculate the Riemann mean

Step 1. Input $\mathbf{R}_q(q = 1, 2, \ldots, Q)$ and τ.

Step 2. Calculate the gradient of the objective function

$$\nabla f = \sum_{q=1}^{Q}\log(\overline{\mathbf{R}}_h^{-\frac{1}{2}}\mathbf{R}_q^{\frac{1}{2}}\overline{\mathbf{R}}_h^{-\frac{1}{2}}). \tag{24}$$

Step 3. $\overline{\mathbf{R}}_{h+1}$ is calculated by (23).

Step 4. Update the numbers of iteration $h = h + 1$.

Step 5. Output $\overline{\mathbf{R}}(\overline{\mathbf{R}} = \overline{\mathbf{R}}_{h+1})$ if the algorithm converges; otherwise it continues.

C. EXTRACT SIGNAL FEATURE VECTORS

In this section, we will introduce how to extract a two-dimensional signal feature vector. Firstly, SUs collect the noise signal and perform PCA when the PU signal is absent. Moreover, the received signal is divided into $\mathbb{Y}_{w1}$ and $\mathbb{Y}_{w2}$ in the FC, and $\mathbf{R}^{w1}$ and $\mathbf{R}^{w2}$ are gained. Similarly, these above steps are performed many times and multiple matrices, $\mathbf{R}_i^{w1}$ and $\mathbf{R}_i^{w2}$, can be obtained. Furthermore, all $\mathbf{R}_i^{w1}$ and $\mathbf{R}_i^{w2}$ are mapped to the statistical manifold. Indeed, the Riemann mean $\overline{\mathbf{R}^{w1}}$ and $\overline{\mathbf{R}^{w2}}$ are given by *Algorithm 2*, respectively.

Next, SUs observe the authorized channel and collect signal. After PCA, the main signal is sent to the FC. And then, the covariance matrices, $\mathbf{R}_1$ and $\mathbf{R}_2$, are obtained and mapped onto the statistical manifold. According to the binary hypothesis of spectrum sensing, the distribution of covariance matrix $\mathbf{R}_{z(z=1,2)}$ on the manifold is similar to the distribution of $\overline{\mathbf{R}^{wz}}$ when the PU signal is absent; otherwise, the distribution of $\mathbf{R}_z$ is different from the distribution of $\overline{\mathbf{R}^{wz}}$. Thus, the state of a PU can be detected by this difference. Significantly, using

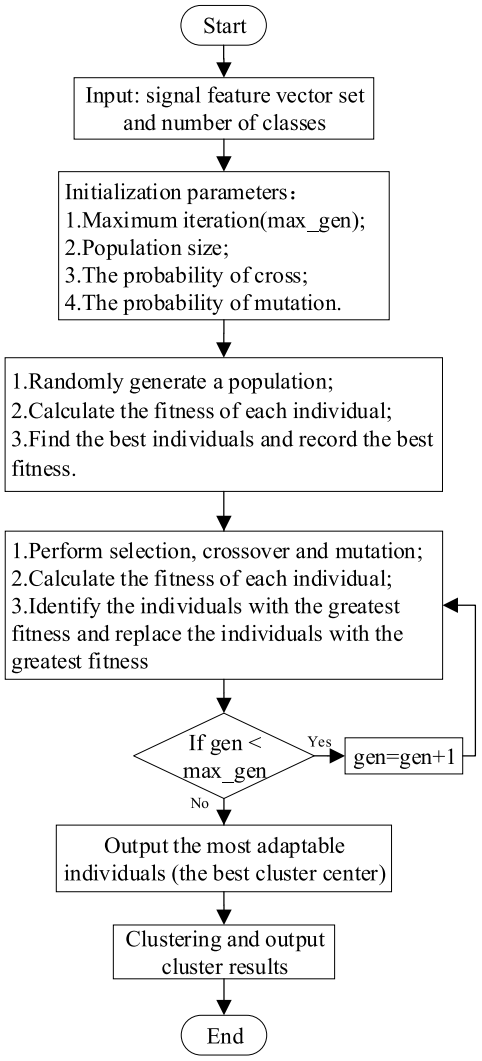

FIGURE 3. These basic steps of the GAC algorithm.

$\overline{\mathbf{R}^{wz}}$ as a reference point, the Riemann distance d_1 and d_2 are calculated by (19). d_1 and d_2 are given by

$$d_1 = \mathcal{D}^2(\overline{\mathbf{R}^{w1}}, \mathbf{R}_1) \tag{25}$$

and

$$d_2 = \mathcal{D}^2(\overline{\mathbf{R}^{w2}}, \mathbf{R}_2), \tag{26}$$

respectively.

As a result, a two-dimensional signal feature vector, $T = [d_1, d_2]$, can be obtained. How to use signal feature vectors to train the GAC model will be described in Section V.

V. SPECTRUM SENSING BASED ON GAC ALGORITHM

How the GAC algorithm works will be presented in this section. It is also one of vitally steps for the MIEGAC to make a precise decision. And these basic steps of the GAC algorithm are described in Fig. 3 [33].

It is key that the FC fits in the GAC model well. Firstly, a feature set $\widehat{T}$ that has enough signal feature vectors tend

to be needed, which is used to train the GAC model. Then, the parameters of the GAC algorithm are initialized, such as maximum iteration, population size, the probability of cross and the probability of mutation. Moreover, the fitness is calculated and the best fitness is record, after selection and crossover as well as mutation are carried out [32]. Finally, the GAC model is gained when maximum iteration is satisfied. Interestingly, the GAC model is successfully trained, two cluster centers with the best clustering effect are obtained. A classifier based on these cluster centers can directly detect the state of a PU. And the mathematical model of the classifier can be written as

$$\Upsilon(T_i) = \frac{\|T_i - \Psi_1\|}{\min_{k=2,3,\ldots,k} \|T_i - \Psi_k\|} \geq \vartheta, \tag{27}$$

where $\widehat{T}$ indicates feature vector set, $\widehat{T} = [T_1, T_2, \ldots, T_i]$; Ψ_k denotes the centroid and k represents the number of classes; ϑ is a parameter that controls the probability of missed detection (P_m) and the probability of false alarm (P_f). If $\Upsilon(T_i) \geq \vartheta$, it means that the PU signal is present and the authorized channel is unavailable. Otherwise, it denotes the PU signal is absent and the authorized channel is available. The GAC model doesn't train again after it is obtained. Apparently, this model can be directly used to detect the state of a PU next time.

VI. SIMULATION RESULTS AND ANALYSIS

Simulation results of the MIEGAC are described here, where the performance of the MIEGAC is evaluated and discussed according to the experiment results. It is noted that two conditions are considered in the simulations. One is that SU collects the sensing signal with the same SNR. Another condition is that SU gains the observed signal with a different SNR, owing to every SU has a different location. In Section VI-A, therefore, the parameters of the MIEGAC are discussed; and the MIEGAC is evaluated whether it has the best performance than some popular sensing algorithms in Section VI-B.

Suppose that the PU signal is AM signal under the ideal Gaussian white noise. To show the experiment results well, a feature set $\widehat{T} = [\widehat{T}_1, \widehat{T}_2, \ldots, \widehat{T}_{2000}]$ formed by 2000 signal features is to train the GAC model and a feature set $\widetilde{T} = [\widetilde{T}_1, \widetilde{T}_2, \ldots, \widetilde{T}_{5000}]$ formed by 5000 signal features is to evaluate the sensing performance of the classifier. Assume that both feature sets, $\widetilde{T}$ and $\widehat{T}$, have two status of the PU signal (H_1 and H_0).

A. PERFORMANCE ANALYSIS OF THE MIEGAC WITH DIFFERENT PARAMETERS

The impact of parameters on the MIEGAC performance is discussed here, such as the parameter β, number of antennas L and number of SUs M. It is known that the evaluation of spectrum sensing performance is mainly measured by (P_f) and the probability of detection (P_d) [20]. Firstly, the impact of parameter β on the MIEGAC performance is analyzed. And simulation results of different β are displayed in Fig. 4, Fig. 5 and Fig. 6.

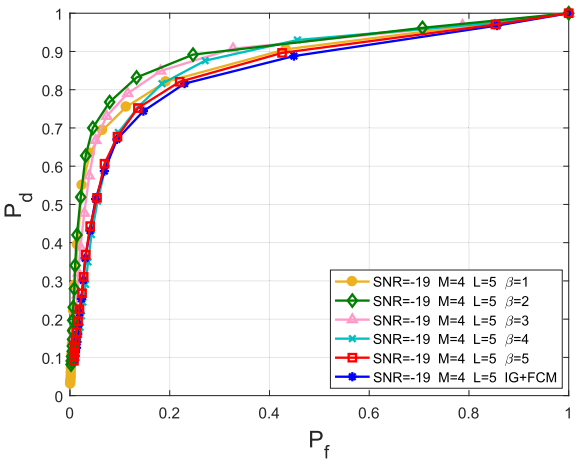

FIGURE 4. The ROC curves under different β and SNR = −19 dB.

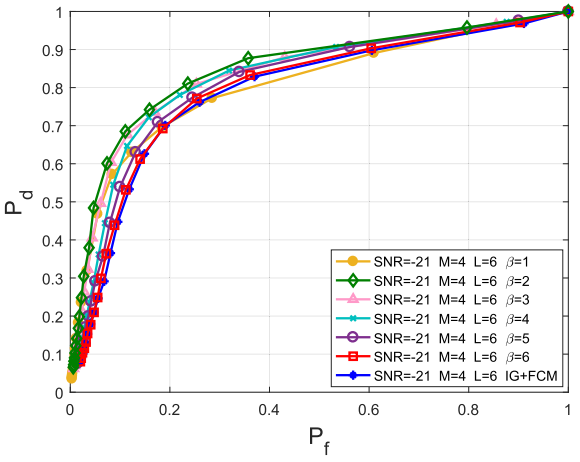

FIGURE 5. The ROC curves under different β and SNR = −21 dB.

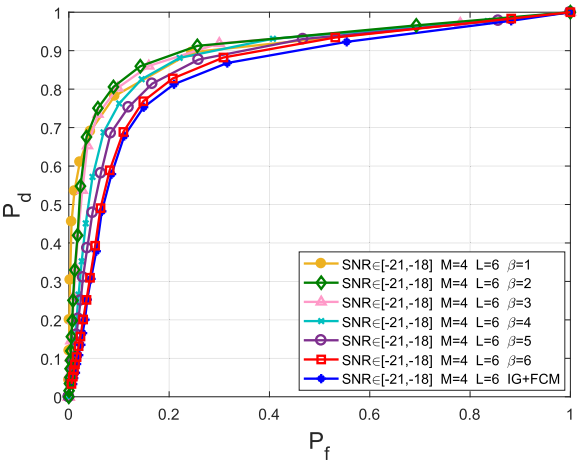

FIGURE 6. The ROC curves under different β and SNR ∈ [−21, −18].

As can be apparently seen in Fig. 4 and Fig. 5, no matter what the value of β is, the MIEGAC always works better than the scheme based on information geometry (IG) and Fuzzy-c-means clustering algorithm (FCM) [23] when SNR

is identical. And simulation results also show that the GAC algorithm has better detection performance than FCM when $\beta = L$. Less main signal is transmitted to the FC and the MIEGAC has poor performance when $\beta = 1$, as a lot of both useful signal and interfering signal are rejected after PCA. And the FC can't make a accurate decision by a small amount of signal. Moreover, all the sensing signal is transmitted to the FC when $\beta = L$. And it doesn't make the FC to make accurate decisions, too. Clearly, it is concluded from the above ROC curves that the MIEGAC has the best performance when $\beta = 2$, because enough the main signal is extracted and a lot of interfering signal is rejected.

It is suggested from Fig. 6 that the MIEGAC also works better than the scheme based on IG and FCM when SNR of SUs are -18 dB, -19 dB, -20 dB and -21dB, respectively. Surprisingly, under SNR of SUs are different, the MIEGAC work well when $\beta = 2$, too. Given what has been analyzed above, the MIEGAC has good performance when $\beta = 2$. Furthermore, the MIEGAC works better than the algorithm based on IG and FCM.

Next, it should be analyzed whether the MIEGAC has different performance when L is different. The ROC curves of the MIEGAC with different L are given in Fig. 7 under $\beta = 2$, $M = 6$ and SNR $= -20$ dB. As can be clearly seen in Fig. 7, the MIEGAC has poor performance where $L = 1$, but it has the best performance where $L = 8$. For multi-antenna technology, it can make full use of spatial multiplexing and spatial diversity to improve the sensing performance. Thus, the MIEGAC could work well when many antennas observe the authorized channel together.

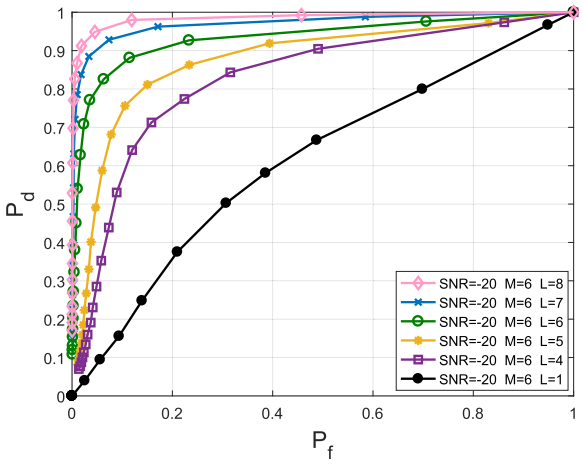

FIGURE 7. The ROC curves under different L and SNR $= -20$ dB.

Finally, the sensing performance with different M is tested when $\beta = 2$, $L = 5$ and SNR $= -21$ dB. And simulation results are presented in Fig. 8. Obviously, the MIEGAC works well when $M = 14$. However, it has relatively terrible performance when $M = 6$. The MIEGAC performance is improved when many SUs participate in spectrum sensing together, since the spatial diversity is exploited through cooperative sensing technology.

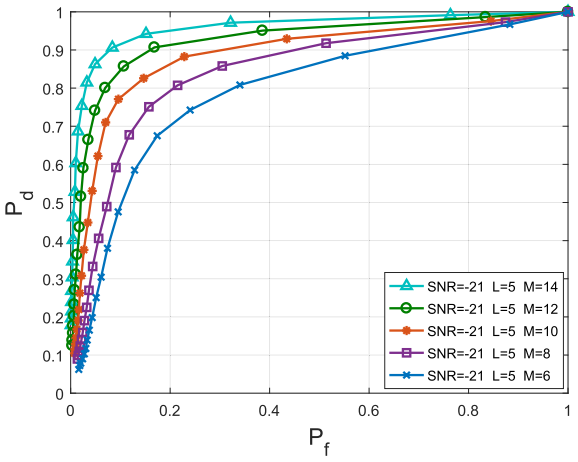

FIGURE 8. The ROC curves under different M and SNR $= -21$ dB.

In a word, the MIEGAC has the best detection performance when $\beta = 2$. And it reduces the cost of the reporting channel when $l > 2$ and $\beta < l$, because a lot of interfering signal is eliminated. Besides, it also works better when SU has more antennas or more SUs participate in spectrum sensing.

B. PERFORMANCE COMPARISON OF THE MIEGAC AND OTHER ALGORITHMS

In this part, simulations results are used to compare the MIEGAC with some popular algorithms. Firstly, a feature set $\widehat{T}$ is obtained under SNR $= -13$ dB, $\beta = 2$, $M = 2$, $L = 3$. And all elements in the set $\widehat{T}$ can be represented on a two-dimensional plane, as shown in Fig. 9. After the GAC model is successfully trained by the set $\widehat{T}$, the classification effect could be observed in Fig. 10. Apparently, the distance on the manifold between the feature vectors and the reference point is small when the PU signal is absent, since the reference point is the Riemann mean calculated by the noise signal features. On the contrary, the distance is large. Given what has been explained above, Ψ_1 indicates the noise signal centroid and Ψ_2 denotes the PU signal centroid, as shown in Fig. 10.

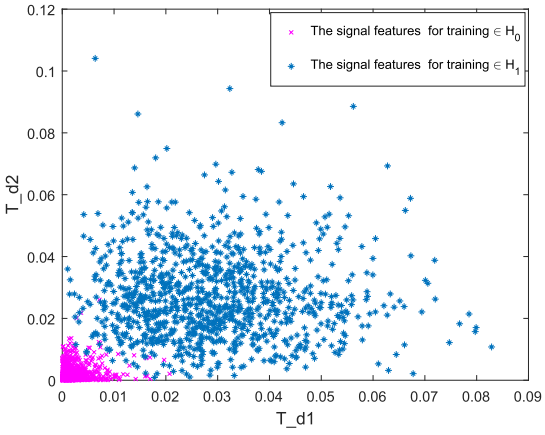

FIGURE 9. The picture of the training signal features.

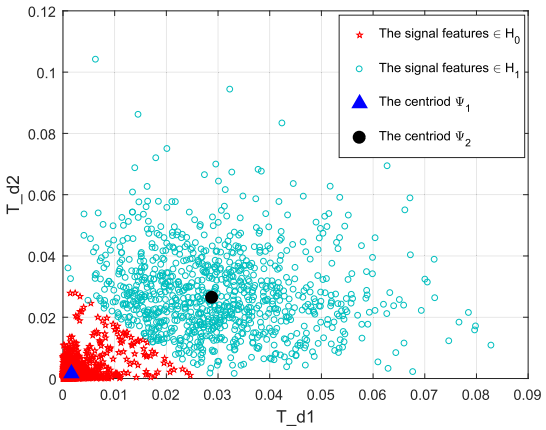

FIGURE 10. The clustering drawing.

Specifically, the MIEGAC is compared with some published algorithms [20], such as the difference of maximum and average eigenvalue (DMAE), the difference between maximum and minimum eigenvalue (DMM), the ratio of maximum eigenvalue to the trace (RMET), the ratio of maximum and minimum eigenvalue (MME). And simulation results are drawn in Fig. 11 and Fig. 12.

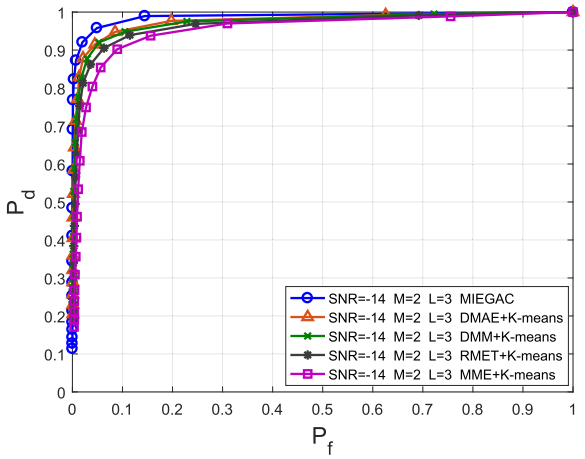

FIGURE 11. The MIEGAC vs different algorithms under SNR = −14dB.

Undoubtedly, simulation results reveal that the MIEGAC works better than other algorithms when SNR of SUs are identical, as it takes great advantage of the received signal information through information geometry and removes a lot of interfering information through PCA. While the MIEGAC performance is relatively close to others when SNR = −14 dB, the MIEGAC has the best performance. Notably, the MIEGAC performance is significantly better than others when SNR = −16 dB. Thus, it is stated that the MIEGAC can work well at low SNR.

In Fig. 13, SNR of SUs are −18 dB, −17 dB, −16 dB and −15 dB, respectively. And in Fig. 14, SNR of SUs are −21 dB, −19 dB, −17 dB and −15 dB, respectively. According to the above ROC curves that are shown in Fig. 13 and Fig. 14, it is easily job for us to conclude that the MIEGAC has markedly better performance than other schemes when SNR of SUs are different.

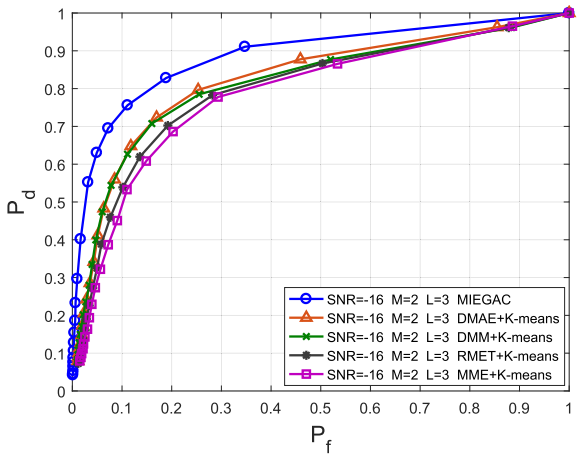

FIGURE 12. The MIEGAC vs different algorithms under SNR = −16dB.

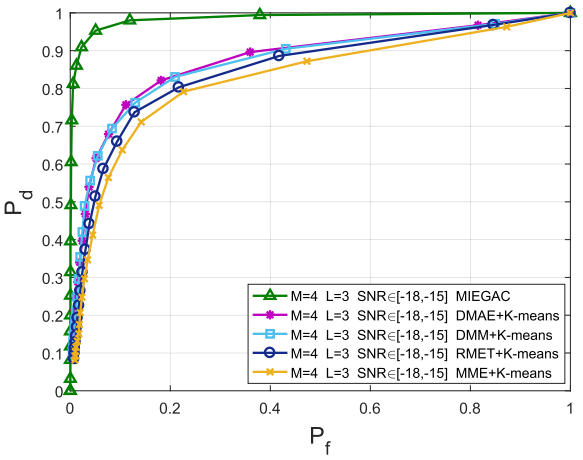

FIGURE 13. The MIEGAC vs different algorithms under SNR ∈ [−18, −15].

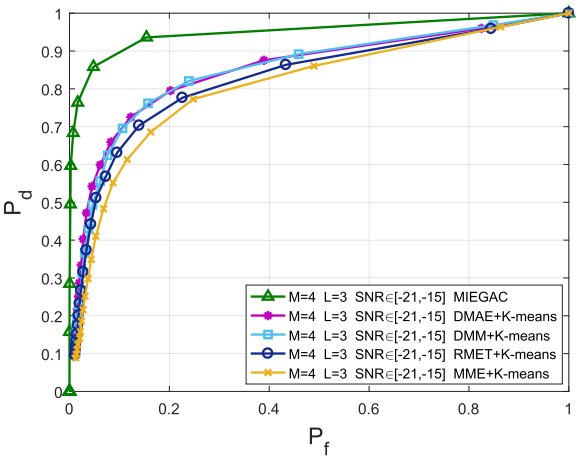

FIGURE 14. The MIEGAC vs different algorithms under SNR ∈ [−21, −15].

To sum up, the MIEGAC improves spectrum sensing performance under the condition that SNR of SUs are identical or different.

VII. CONCLUSION

Aim at improving the sensing performance, a multi-antenna spectrum sensing scheme based on main information extraction and genetic algorithm clustering is proposed in this

paper. Specifically, a scheme based on PCA is proposed to reduce the cost of the reporting channel, since β can control the amount of the main signal that is transmitted to the FC. And a lot of interfering signal is filtered after PCA. According to the simulation results, the impact of parameter β on the sensing performance is discussed and the MIEGAC has the best sensing performance when $\beta = 2$. Moreover, an information fusion method is described, which avoids IQ and DAR. Furthermore, a decision method based on the GAC algorithm is presented to improve the sensing accuracy. Particularly, it is considered in the simulations that SU gains the observed signal with a different SNR. Eventually, all simulation results reveal that the MIEGAC can work better than recently popular spectrum sensing methods.

REFERENCES

[1] G. Chu, K. Niu, W. Wu, and F. Yang, "MGF-based analysis of spectrum sensing over K—μ fading channels for 5G cognitive networks," *IEEE Access*, vol. 6, pp. 78650–78658, 2018.

[2] H. Ding, Y. Fang, X. Huang, M. Pan, P. Li, and S. Glisic, "Cognitive capacity harvesting networks: Architectural evolution toward future cognitive radio networks," *IEEE Commun. Surveys Tuts.*, vol. 19, no. 3, pp. 1902–1923, 3rd Quart., 2017.

[3] F. Hu, B. Chen, and K. Zhu, "Full spectrum sharing in cognitive radio networks toward 5G: A survey," *IEEE Access*, vol. 6, pp. 15754–15776, 2018.

[4] X. Huang and M. Dai, "Indoor device-free activity recognition based on radio signal," *IEEE Trans. Veh. Technol.*, vol. 66, no. 6, pp. 5316–5329, Jun. 2017.

[5] T. Xiong, Y.-D. Yao, Y. Ren, and Z. Li, "Multiband spectrum sensing in cognitive radio networks with secondary user hardware limitation: Random and adaptive spectrum sensing strategies," *IEEE Trans. Wireless Commun.*, vol. 17, no. 5, pp. 3018–3029, May 2018.

[6] M. Zareei, A. K. M. M. Islam, S. Baharun, C. Vargas-Rosales, L. Azpilicueta, and N. Mansoor, "Medium access control protocols for cognitive radio ad hoc networks: A survey," *Sensors*, vol. 17, no. 9, p. 2136, 2017.

[7] H. Oh and H. Nam, "Energy detection scheme in the presence of burst signals," *IEEE Signal Process. Lett.*, vol. 26, no. 4, pp. 582–586, Apr. 2019.

[8] W. Tian and G. Guo, "Performance comparison between matched filter and locally optimal detector for composite hypothesis test with inaccurate noise," *IET Signal Process.*, vol. 12, no. 2, pp. 163–168, Apr. 2018.

[9] C. Han, B. Ai, L. Yang, and L. Liu, "DF-based cooperative spectrum sensing in multi-antenna cognitive radio network," in *Proc. 5th IET Int. Conf. Wireless, Mobile Multimedia Netw. (ICWMMN)*, Nov. 2013, pp. 145–149.

[10] P. Petropoulou, E. T. Michailidis, A. D. Panagopoulos, and A. G. Kanatas, "Radio propagation channel measurements for multi-antenna satellite communication systems: A survey," *IEEE Antennas Propag. Mag.*, vol. 56, no. 6, pp. 102–122, Dec. 2014.

[11] Y. Wu, C. Xiao, Z. Ding, X. Gao, and S. Jin, "A survey on MIMO transmission with finite input signals: Technical challenges, advances, and future trends," *Proc. IEEE*, vol. 106, no. 10, pp. 1779–1833, Oct. 2018.

[12] D. Seo and H. Nam, "A parallel multi-Channel cooperative spectrum sensing in cognitive radio networks," in *Proc. Int. Symp. Antennas Propag. (ISAP)*, Oct. 2018, pp. 1–2.

[13] K. Bouallegue, I. Dayoub, M. Gharbi, and K. Hassan, "Blind spectrum sensing using extreme eigenvalues for cognitive radio networks," *IEEE Commun. Lett.*, vol. 22, no. 7, pp. 1386–1389, Jul. 2018.

[14] Y. Lei, Y. Qiang, and D. Weibo, "Matrix constant false alarm rate (MCFAR) detector based on information geometry," in *Proc. IEEE Inf. Technol., Netw., Electron. Automat. Control Conf.*, May 2016, pp. 211–215.

[15] Q. Chen, P. Wan, Y. Wang, J. Li, and Y. Xiao, "Research on cognitive radio spectrum sensing method based on information geometry," in *Proc. Int. Conf. Cloud Comput. Secur.*, Nov. 2017, pp. 554–564.

[16] L. Xiao, Y. Li, J. Liu, and Y. Zhao, "Power control with reinforcement learning in cooperative cognitive radio networks against jamming," *J. Supercomput.*, vol. 71, no. 9, pp. 3237–3257, Sep. 2015.

[17] L. Xiao, J. Liu, Q. Li, N. B. Mandayam, and H. V. Poor, "User-centric view of jamming games in cognitive radio networks," *IEEE Trans. Inf. Forensics Security*, vol. 10, no. 12, pp. 2578–2590, Dec. 2015.

[18] Z. Qu, Y. Xu, and S. Yin, "A novel clustering-based spectrum sensing in cognitive radio wireless sensor networks," in *Proc. IEEE 3rd Int. Conf. Cloud Comput. Intell. Syst.*, Nov. 2014, pp. 695–699.

[19] V. Kumar, D. C. Kandpal, M. Jain, R. Gangopadhyay, and S. Debnath, "K-mean clustering based cooperative spectrum sensing in generalized $\kappa - \mu$ fading channels," in *Proc. 22nd Nat. Conf. Commun. (NCC)*, Mar. 2016, pp. 1–5.

[20] Y. W. Zhang, P. Wan, Y. Wang, N. Li, and S. Zhang, "A spectrum sensing method based on signal feature and clustering algorithm in cognitive wireless multimedia sensor networks," *Adv. Multimedia*, vol. 2017, Oct. 2017, Art. no. 2895680.

[21] Y. Wang, Y. Zhang, S. Zhang, X. Li, and P. Wan, "A cooperative spectrum sensing method based on a feature and clustering algorithm," in *Proc. Chin. Automat. Congr. (CAC)*, Nov./Dec. 2018, pp. 1029–1033.

[22] S. Zhang, Y. Wang, P. Wan, Y. Zhang, and X. Li, "A cooperative spectrum sensing method based on clustering algorithm and signal feature," in *Proc. Int. Conf. Cloud Comput. Secur.*, Jun. 2018, pp. 50–62.

[23] S. Zhang, Y. Wang, P. Wan, Y. Zhang, X. Li, and J. Li, "A cooperative spectrum sensing method based on information geometry and fuzzy c-means clustering algorithm," *EURASIP J. Wireless Commun. Netw.*, vol. 2019, no. 1, p. 17, Dec. 2019.

[24] Y. Wang, S. Zhang, Y. Zhang, P. Wan, J. Li, and N. Li, "A cooperative spectrum sensing method based on empirical mode decomposition and information geometry in complex electromagnetic environment," *Complexity*, vol. 2019, Feb. 2019, Art. no. 5470974.

[25] W. Jian-Xiang, L. Huai, S. Yue-Hong, and S. Xin-Ning, "Application of genetic algorithm in document clustering," in *Proc. Int. Conf. Inf. Technol. Comput. Sci.*, Jul. 2009, pp. 145–148.

[26] N. Mansoor, A. K. M. M. Islam, M. Zareei, and C. Vargas-Rosales, "RARE: A spectrum aware cross-layer MAC protocol for cognitive radio ad-hoc networks," *IEEE Access*, vol. 6, pp. 22210–22227, 2018.

[27] S. Maleki, S. P. Chepuri, and G. Leus, "Optimal hard fusion strategies for cognitive radio networks," in *Proc. IEEE Wireless Commun. Netw. Conf.*, Mar. 2011, pp. 1926–1931.

[28] K. M. Carter, R. Raich, W. G. Finn, and A. O. Hero, III, "Information-geometric dimensionality reduction," *IEEE Signal Process. Mag.*, vol. 28, no. 2, pp. 89–99, Mar. 2011.

[29] P.-R. Lin, Y.-Z. Chen, P.-H. Chang, and S.-S. Jeng, "Cooperative spectrum sensing and optimization on multi-antenna energy detection in Rayleigh fading channel," in *Proc. 27th Wireless Opt. Commun. Conf. (WOCC)*, Apr./May 2018, pp. 1–5.

[30] M. Jin, Y. Li, and H.-G. Ryu, "On the performance of covariance based spectrum sensing for cognitive radio," *IEEE Trans. Signal Process.*, vol. 60, no. 7, pp. 3670–3682, Jul. 2012.

[31] Q. Zhang and Y.-W. Leung, "A class of learning algorithms for principal component analysis and minor component analysis," *IEEE Trans. Neural Netw.*, vol. 11, no. 2, pp. 529–533, Mar. 2000.

[32] Q. Lu, S. Yang, and F. Liu, "Wideband spectrum sensing based on Riemannian distance for cognitive radio networks," *Sensors*, vol. 17, no. 4, p. 661, Mar. 2017.

[33] A. Ebrahimzadeh and M. Hossienzadeh, "A novel method using GA-based clustering and spectral features for modulation classification," in *Proc. Int. Conf. Elect. Control Eng.*, Sep. 2011, pp. 4705–4708.

JIAWEI ZHUANG received the B.S. degree from Jiaying University, in 2017. He is currently pursuing the M.S. degree with the Guangdong University of Technology, Guangdong, China. His research interest includes spectrum sensing in cognitive radio.

YONGHUA WANG received the B.S. degree in electrical engineering and automation from the Hebei University of Technology, in 2001, the M.S. degree in control theory and control engineering from the Guangdong University of Technology, in 2006, and the Ph.D. degree in communication and information system from Sun Yat-sen University, in 2009. He is currently an Associate Professor with the School of Automation, Guangdong University of Technology, Guangdong, China. He is also with the State Key Laboratory of Management and Control for Complex Systems, Institute of Automation, Chinese Academy of Sciences, Beijing, China.

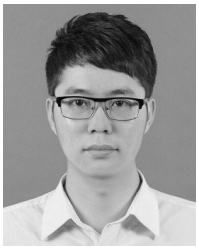

SHUNCHAO ZHANG received the B.S. degree from the Hunan Institute of Engineering, in 2016. He is currently pursuing the M.S. degree with the Guangdong University of Technology, Guangdong, China. His research interest includes spectrum sensing in cognitive radio.

PIN WAN received the B.S. degree in electronic engineering from Southeast University, in 1984, the M.S. degree in circuit and system from Southeast University, in 1990, and the Ph.D. degree in control theory and control engineering from the Guangdong University of Technology, in 2011. He currently is a Professor with the School of Automation, Guangdong University of Technology, Guangdong, China. He is currently a Professor with the School of Automation, Guangdong University of Technology, Guangdong, China. He is also with the Hubei Key Laboratory of Intelligent Wireless Communications, South-Central University for Nationalities, Wuhan, China.

CHENHAO SUN received the B.S. degree from Zhoukou Normal University, in 2015. He is currently pursuing the M.S. degree with the Guangdong University of Technology, Guangdong, China. His research interest includes spectrum sensing in cognitive radio.